DOI 10.31489/2020Ph2/7-17

UDC 621.793:621.785.532

A.S. Rudenkov[1], A.V. Rogachev[1], S.M. Zavadski[2], D.A. Golosov[2], P.A. Luchnikov[3], G.Yu. Dalskaya[3], A.N. Vtoruchina[4]

[1]Francisk Skorina Gomel State University, Gomel, Belarus;
[2]Belarusian State University of Informatics and Radioelectronics, Minsk, Belarus;
[3]MIREA – Russian Technological University, Moscow, Russia;
[4]National Research Tomsk Polytechnic University, Tomsk, Russia
(E-mail: xamdex@gmail.com)

Nitrided Silicon-Carbon Coatings Structure and Properties

The paper considers structural and physicomechanical properties of silicon-carbon coatings deposited from a gaseous medium in doping with nitrogen ions. The analysis of the coatings by X-ray photoelectron spectroscopy shows that nitriding of silicon-carbon coatings promotes the formation of silicon nitride and compounds such as CN_x and $Si_xO_yN_z$. A 1.5–2-fold increase in the content of sp^2-hybridized carbon and silicon carbide atoms is found to prevent silicon oxidation. Thermal annealing of the resulting silicon-carbon coatings increases the content of the graphite phase and silicon oxide.It is shown that doping of the working gas with nitrogen ($Ar_{57\,\%} + N_{43\,\%}$) leads to the formation of a more finely dispersed structure as compared to that when using argon only. During thermal annealing in air, the decreased carbon concentration and increased oxygen concentration can be observed due to silicon and carbon oxidation followed by desorption of carbon and oxygen compounds. In addition, annealing leads to nitrogen desorption from the coating. Nitriding of silicon-carbon coatings increases the dispersion of their structure, and heat-resistant compounds CN_x, Si_3N_4 improve heat resistance and thermal stability of coatings, and increase microhardness and friction coefficient in friction units.

*Keywords***:** carbon coatings, nitriding, silicon, phase composition, ion beam sputtering, Raman spectroscopy, XPS, microhardness, friction coefficient.

Introduction

In the general case, the properties of carbon coatings and their dependence on the synthesis parameters are determined by the polymorphism of the structural configurations of carbon in both crystalline and amorphous states [1–5]. Ion nitriding of nanosized carbon-based coatings is an effective technological technique that allows controlling their phase structure during the deposition process [6, 7]. Silicon alloying is one of the most effective methods for increasing the heat resistance of carbon coatings [8]. Thus, the study of chemical interaction processes which occur during the deposition of silicon-carbon coatings by ion-beam sputtering of a silicon carbide target using a mixture of nitrogen and argon as a working gas and which lead to the formation of solid carbide and nitride phases is a vital task. Solving this problem will allow us to develop effective technological methods for the formation of coatings that will be characterized by high heat resistance properties.

The aim of this article is to study the influence of nitriding on the structure and mechanical properties of silicon-carbon coatings deposited by ion-beam sputtering of a silicon carbide target during the formation process and subsequent thermal treatment.

Samples and research methods

Silicon-carbon coatings were formed by ion beam sputtering of a silicon carbide target. The power of the ion source was 738 W ($I_{of\ discharge}$=164 mA, $U_{of\ discharge}$ = 4,5 kV, $I_{of\ target}$= 174 mA), the coating thickness was (270±10) nm. Nitrogen was brought in the working gas for coating nitriding. The volume content of argon was 57 %, and the nitrogen content was about 43 %. The coatings were being annealed in the air at a temperature of 600 °C and 700 °C for 30 minutes.

Silicon-carbon coatings morphology was studied by atomic force microscopy method (AFM) in the modes of topography measuring and phase contrast using a Solver Pro device manufactured by NT-MDT (Moscow, Russia). Sections of 4x4 μm^2 in size were scanned. The coatings chemical structure was determined by X-ray photoelectron spectroscopy (XPS) method. The measurements were carried out using a PHI Quantera device when the substance was excited with aluminum Kα-radiation with quantum energy of 1486.6 eV and a total power of 250 W. The error in determining the concentration of elements was ± 1 atom per cent. The hydrophobic properties of silicon-carbon coatings were determined by measuring the limiting wetting angle and by calculating the surface energy and its components. The microhardness of silicon-carbon coatings was measured by Knupp method using a DM-8 microhardness tester (AFFRI, Italy). The indenter load was 490 mN. Tribotechnical tests were carried out according to the «sphere-plane» scheme under load of 980 mN, the average indenter movement speed was 0.017 m/s.

Results and Their Discussion

It is given that the size of individual structural features (grains) of silicon-carbon coatings is larger and the grain which was carried out in the presence of nitrogen and argon in the working gas structure. When the annealing temperature of nitrided silicon-carbon coatings is increased, the average height of individual structural features is decreased and their average diameter is slightly decreased as well as the coating dispersion is increased. Annealing of non-nitrided coatings is also accompanied by a decrease in the average height of grains (by 4.7 times) but it occurs in combination with an increase in their average diameter and a decrease in dispersion. Most likely, this is due to graphite clusters merging.

The comparative analysis (Table 1) of non-nitrided and nitrided silicon-carbon coatings elemental structure showed that when nitrogen is brought into the working gas, the concentration of silicon and carbon is slightly lower in comparison with non-nitrided coatings. The influence of annealing in the air on the elemental structure of both types of coatings is similar: there is a decrease in carbon concentration and an increase in oxygen concentration; it is due to silicon and carbon oxidation that is followed by desorption of carbon and oxygen compounds. It was shown that annealing leads to nitrogen desorption, its content decreases by 4 times. Apparently, nitrogen remains in a bound state in the form of CN_x or Si_3N_4 compounds after annealing. These compounds are characterized by high heat resistance [9–11].

Table 1

Chemical structure of non-nitrided and nitrided silicon-carbon coatings

Coating	Temperature, °C	Working gas	Concentration of elements, at. %			
			C	Si	O	N
C+Si	–	$Ar_{100\ \%}$	40.3	25.7	34.0	0.0
		$Ar_{57\ \%}+N_{43\ \%}$	37.1	23.2	31.5	8.6
	600	$Ar_{100\ \%}$	22.3	25.7	52.0	0.0
		$Ar_{57\ \%}+N_{43\ \%}$	22.5	23.2	51.3	3.0
	700	$Ar_{100\ \%}$	20.2	25.7	54.1	0.0
		$Ar_{57\ \%}+N_{43\ \%}$	17.3	23.2	57.4	2.1

In general, the following two-phase carbon peak model is distinguished: phase 1 corresponds to the sp^2 matrix, which includes sp^3-hybridized carbon atoms, and is determined by the D-peak between 1300 cm^{-1} and 1500 cm^{-1}; phase 2 means sp^2 clusters and is determined by G-peak about 1580 cm^{-1} [9]. The analysis of the width of these peaks, changes in their position and intensity ratios gives an idea of the degree of carbon-based coatings ordering, the number and size of clusters with sp^2 bonds.

It is well-known [12], that the ratio of the intensities of the D- and G-peaks is in inverse proportion to the size of the sp^2 clusters: $\frac{I_D}{I_G} = \frac{c(\lambda)}{L_a}$, (1)

where I_D and I_G are the intensities of the correspondent peaks; L_a is the size of graphite grains (nm); $c(\lambda)$ is the proportionality coefficient depending on the wavelength of the exciting radiation (nm).

Table 2

Influence of annealing temperature and working gas structure on the morphological features of silicon-carbon coatings

Coating	Annealing temperature, °C	Working gas	Average height, nm	Rms, nm	Average diameter of grains, nm
C+Si	–	$Ar_{100\,\%}$	5.0	0.6	44
		$Ar_{57\,\%}+N_{43\,\%}$	11.0	0.4	57
	600	$Ar_{100\,\%}$	4.0	1.8	140
		$Ar_{57\,\%}+N_{43\,\%}$	3.9	0.3	53
	700	$Ar_{100\,\%}$	3.7	2.3	166
		$Ar_{57\,\%}+N_{43\,\%}$	2.3	0.5	51

Taking into account the ratio (1), the analysis of Raman spectroscopy results (Table 3) shows that the size of sp^2 clusters in nitrided silicon-carbon coatings is larger than in non-nitrided ones. This conclusion is confirmed by the results of atomic force microscopy (Table 2).

Table 3

Statistical analysis of Raman spectroscopy results

Coating	Working gas	D-peak		G-peak		I_D/I_G
		Position, cm^{-1}	Width, cm^{-1}	Position, cm^{-1}	Width, cm^{-1}	
C+Si	$Ar_{100\,\%}$	1408.9	117.0	1487.3	117.9	1.78
	$Ar_{57\,\%}+N_{43\,\%}$	1427.7	166.9	1513.9	153.2	1.36

The Raman spectra of nitrided silicon-carbon coatings exposed to thermal treatment in the air could not be reliably analyzed due to the high noise level. It is well-known that the coatings based on nitride or silicon oxide and containing silicon clusters have luminescent properties [13]. After thermal treatment the carbon concentration decreases almost by 2 times and the carbon input to the Raman spectrum does not exceed the silicon input and its components, which leads to an increase in the luminescence influence, causing distortion of the spectra. This phenomenon indirectly confirms the presence of SiN_x compounds in the coating, which are characterized by stronger luminescent properties than silicon oxide. It is confirmed by Raman spectroscopy results since the level of distortion in the case of annealing of non-nitrided samples of silicon-carbon coatings is not so significant. The mathematical processing of the above spectra confirms the presence of D- and G-peaks. But they can't be compared with the spectra of non-nitrided silicon-carbon coatings. In addition, the peak was detected at the level of 2250 cm^{-1}. This peak can correspond to the compound of CN_x type or simply be an overton of D- and G- peaks.

The detailed analysis of the results of XPS of silicon-carbon coatings formed by ion-beam sputtering of silicon carbide was given by us earlier in the article [8].

There are several methods for the C1s peak decomposition of XPS of nitrogen-containing carbon coatings. In [14] the C1s peak is decomposed into four components: Csp^2 ~ 284.5 eV, Csp^2–N ~ 286.6 eV, Csp^3–N ~ 287.3 eV and C=O ~ 290 eV. The author of [15] mean C–N and C=N bonds by components with a binding energy of 285÷286 eV and 287 eV, respectively, and they compare 288 eV to β-C_3N_4. The authors of [16] divide the C1s peak into three and correlate the component with a binding energy of 285–286 eV with sp^3-hybridized carbon atoms and C — N, C = N. Due to such an ambiguity in the determination of CN_x bonds and a low nitrogen concentration in the coating the Csp^3 compound of the C1s peak is combined with the component related to the C — N, C = N bonds.

C–Si with binding energy ~ 283.6 eV [17] Csp^2 ~ 284.4 eV, Csp^3 and CN_x ~ 285.5 eV, C–O ~ 286.5 eV [8] were identified in the C1s peak of nitrided silicon-carbon coatings (Fig. 1).

In addition to the above specified components of the Si2p peak, nitrided silicon-carbon coatings are characterized by the presence of a component near 101.7 ÷ 102 eV (Fig. 2), which corresponds to the Si N bond (Si_3N_4) [18]. The values of Si-N binding energy are close to values of C–Si–O binding energy (101.7 eV) [19], therefore, these components were combined into one during the decomposition of Si2p peak.

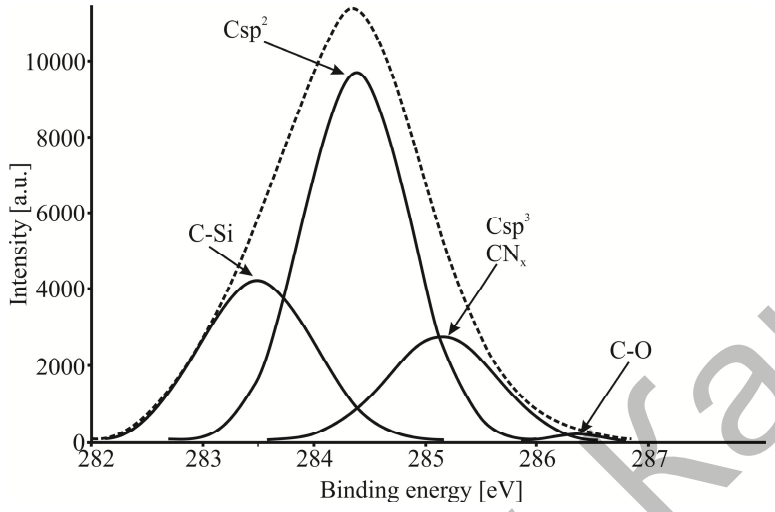

Figure 1. C1s peak of XPS of nitrided silicon-carbon coatings

In addition, during the decomposition of the Si2p peak the nitrided silicon-carbon coatings are characterized by the occurrence of a component with the binding energy of 102.4÷102.8 eV corresponding to the O — Si — N bond [20].

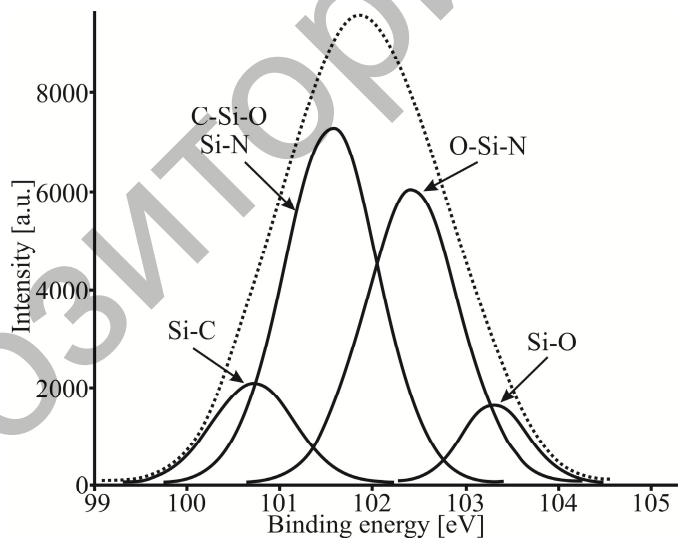

Figure 2. Si2p peak of XPS of nitrided silicon-carbon coatings

Making Si-N bonds during the formation of silicon-carbon coatings using a gas mixture of $Ar_{57\,\%}$ + $N_{43\,\%}$ is also confirmed by analysis of the N1s peak. Bond N-Si in the N1s peak is detected near 397÷398 eV [19, 20], bond of nitrogen atoms with sp^2- hybridized carbon atoms is determined at the level of 399 eV, and with sp^3-hybridized — near 399.9 eV [21]. Bond Si-O-N is determined close to 400 eV [22], these components of N1s peak were combined due to their proximity to N-Csp^2. The decomposition of the N1s peak was made as follows (Fig. 3): N-Si with binding energy 397.6 eV, N-Csp^3~398.7 eV, N-Csp^2+Si-O-N ~399.9 eV.

Thus, the XPS analysis of nitrided silicon-carbon coatings shows that bringing nitrogen into the working gas structure ($Ar_{57\,\%}$+$N_{43\,\%}$) at ion sputtering of the SiC target leads to the formation of silicon nitride and compounds of CN_x and $Si_xO_yN_z$ type. According to the relative input of the integral areas, nitrogen, the component of the N1s peak of XPS, is mainly associated with sp^3- hybridized carbon atoms.

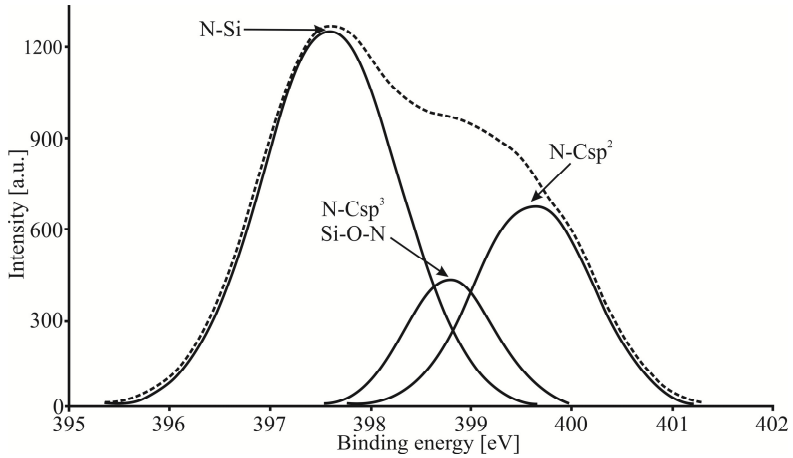

Figure 3. N1s peak of XPS of nitrided silicon-carbon coatings after annealing at 600 °C

If silicon-carbon coatings are formed by bringing nitrogen into the working gas structure, the proportions of the integral area of Csp^2 component of the C1s peak and Si-C component of the Si2p peak is higher, and Si-O component of the Si2p peak are lower than when the coatings are not nitrided (Fig. 4).

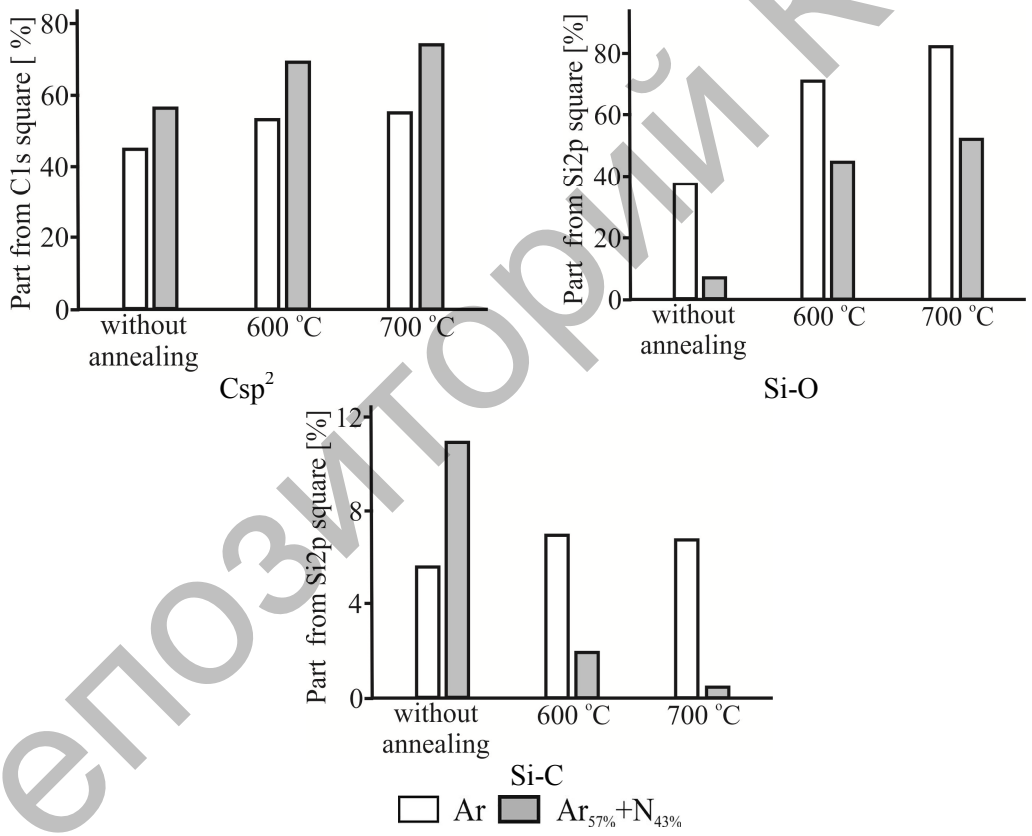

Figure 4. Influence of annealing temperature and nitrogen presence in the working gas on the silicon-carbon coatings structure

Thus, bringing nitrogen into the working gas structure ($Ar_{57\,\%} + N_{43\,\%}$) during the formation of silicon-carbon coatings by ion sputtering of silicon carbide contributes to an increase in the content of sp^2- hybridized carbon atoms and silicon carbide in addition to the formation of silicon nitride and compounds of the CN_x and $Si_xO_yN_z$ type. It also prevents from silicon oxidation.

High-temperature annealing of both non-nitrided and nitrided silicon-carbon coatings leads to an increase in the content of the graphite phase and silicon oxide. Nitrided silicon-carbon coatings annealing

causes intense destruction of silicon carbide, while non-nitrided coatings are characterized by a slight increase in the content of silicon carbide after annealing. Apparently the following happens: annealing causes nitrogen desorption (its content decreases by 4 times (Table 2)), the coating becomes less dense, due to which the oxidation becomes more intense, silicon carbide is destroyed and there occurs the further interaction of silicon and carbon atoms with oxygen and the subsequent desorption of oxygen and carbon compounds. Non-nitrided coatings are probably denser or contain more free silicon atoms, which interact with carbon during annealing, by comparison with the nitrided coatings free silicon atoms interact with nitrogen at the deposition stage.

If the annealing temperature is increased to 700 °C, the proportion of the integral area of N-Si and N-Csp^3 components of the N1s peak of XPS (Fig. 5) is decreased, and at the same time the proportion of integral area of the component which correlates with N-Csp^2 and Si-O-N simultaneously is increased.

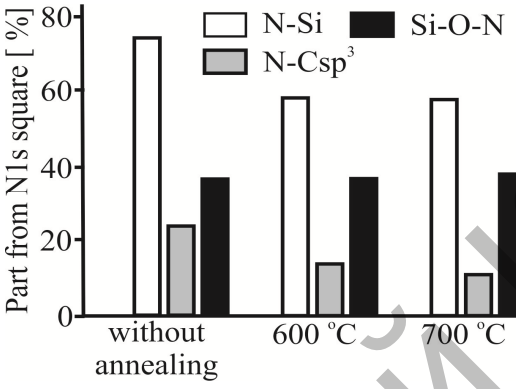

Figure 5. Influence of annealing temperature on the content of N-Si, N-Csp^3 and Si-O-N bonds of nitride silicon-carbon coatings

This increase is explained primarily by the annealing of the $sp^3 \rightarrow sp^2$ phase transitions (Fig. 4), since the increase in the proportion of the integral area of Csp^2 component of the C1s peak is more significant than the change in the proportion of the integral area of Si-O-N component of the Si2p peak (Fig. 5).

We found that heat treatment of non-nitrided silicon-carbon coatings leads to an increase in their surface energy by almost 1.9 times.

After annealing at a temperature of 600°C, the surface energy of silicon-carbon coatings increases, mainly due to an increase in its polar component, which is explained by the $sp^3 \rightarrow sp^2$ phase transition, as well as the formation of strongly polar bonds. With a further increase in the annealing temperature to 700°C, the Si-O-C bonds are destroyed and more stable C-O and Si-O bonds are formed, which leads to a decrease in the polar component of surface energy.

It was found out if nitrogen is brought into the working gas structure at the silicon-carbon coatings deposition by silicon-carbide ion sputtering, the contact angle decreases, and therefore the surface energy decreases (Fig. 6, a, b).

The values of the dispersion component of the surface energy are determined, first of all, by the surface morphology. The dispersion component of nitrided silicon-carbon coatings is higher than that of non-nitrided ones (Fig. 6, c). This is due to their high dispersion structure. The dispersion component of nitrided silicon-carbon coatings changes less significantly after annealing than that of non-nitrided ones. It is completely consistent with the previously obtained results of the analysis of atomic force microscopy data (the surface morphology parameters of nitrided silicon-carbon coatings are practically unchanged).

The values of the polar component of surface energy (Fig. 6, d) of nitrided silicon-carbon coatings are lower than that of non-nitrided coatings. It is explained by a lower content of silicon oxide, since bringing nitrogen into the working gas structure helps to reduce the intensity of oxidizing processes.

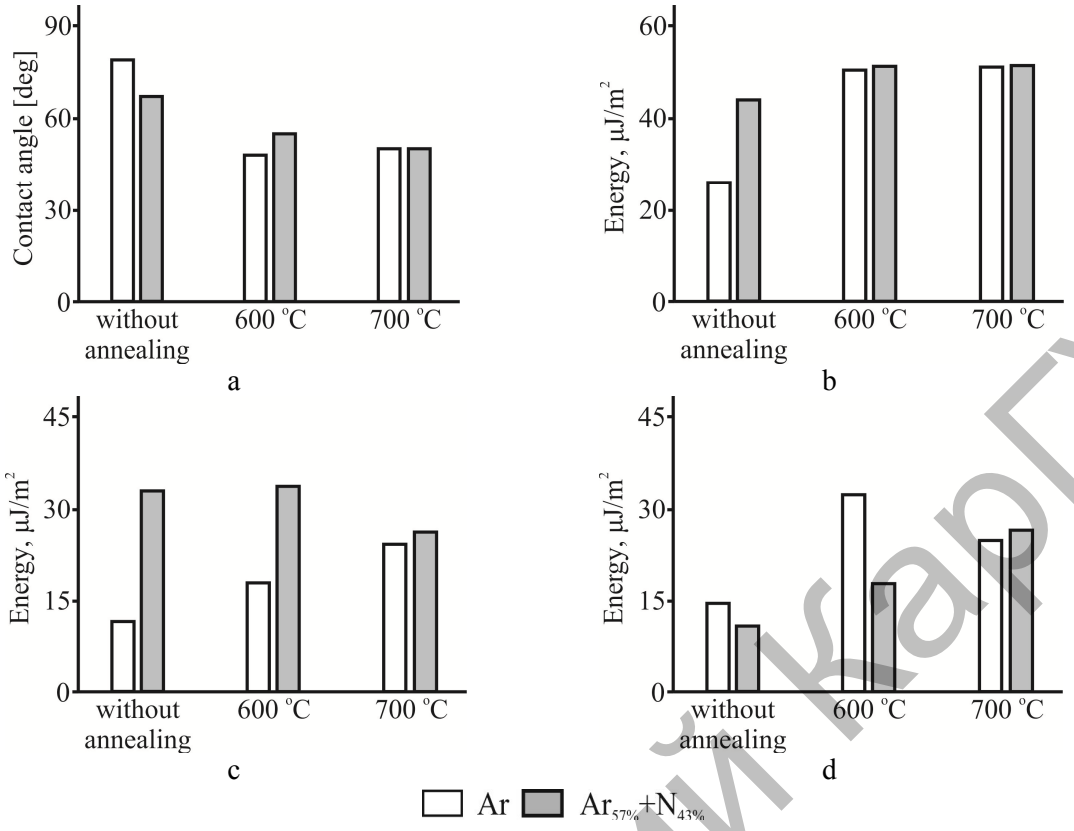

Figure 6. Contact angle (a), total surface energy (b), its dispersion (c) and polar (d) components which characterize the hydrophobic properties of nitrided and non-nitrided silicon-carbon coatings

The total surface energy after annealing in the air raises due to an increase in the polar component both as applied to nitrided and non-nitrided coatings. It is caused by the $sp^3 \rightarrow sp^2$ phase transition, as well as the formation of strongly polar bonds.

Table 4

Influence of thermal treatment parameters on microhardness H_k of nitrided and non-nitrided silicon-carbon coatings and coefficient of volume wear of the counterbody j when interacting with such coatings.

Coating	T, °C	Working gas	H_k, GPa	$j \times 10^{-17}$, $m^3/(N \cdot m)$
C+Si	–	$Ar_{100\,\%}$	13.34±0.25	332±17.3
		$Ar_{57\,\%}+N_{43\,\%}$	10.68±0.15	252±15.1
	600	$Ar_{100\,\%}$	12.05±0.27	185±16.9
		$Ar_{57\,\%}+N_{43\,\%}$	10.86±0.17	302±14.7
	700	$Ar_{100\,\%}$	11.59±0.22	167±14.3
		$Ar_{57\,\%}+N_{43\,\%}$	10.36±0.28	426±15.3

Experimental studies of the microhardness H_k of silicon-carbon coatings (Table 4) showed that it is 10.63 ± 0.2 GPa in nitrided films and 2.7 GPa higher in non-nitrided H_k, i.e. is 12.33 ± 0.2 GPa. This fact is apparently caused by a higher content of sp^2-hybridized carbon atoms in the carbon coating. (Fig. 4).

High-temperature annealing of such coatings, unlike non-nitrided ones, does not cause significant changes in microhardness. It is due to the presence of CN_x and Si_3N_4 compounds in the coating structure, which are characterized by high heat resistance. In addition, according to the Hall-Petch law, a change in microhardness can be caused by a change in the size of sp^2 clusters. According to the previously cited data of atomic force microscopy (Table 1), in the case of nitrided silicon-carbon coatings, the average diameter of individual structural formations varies slightly.

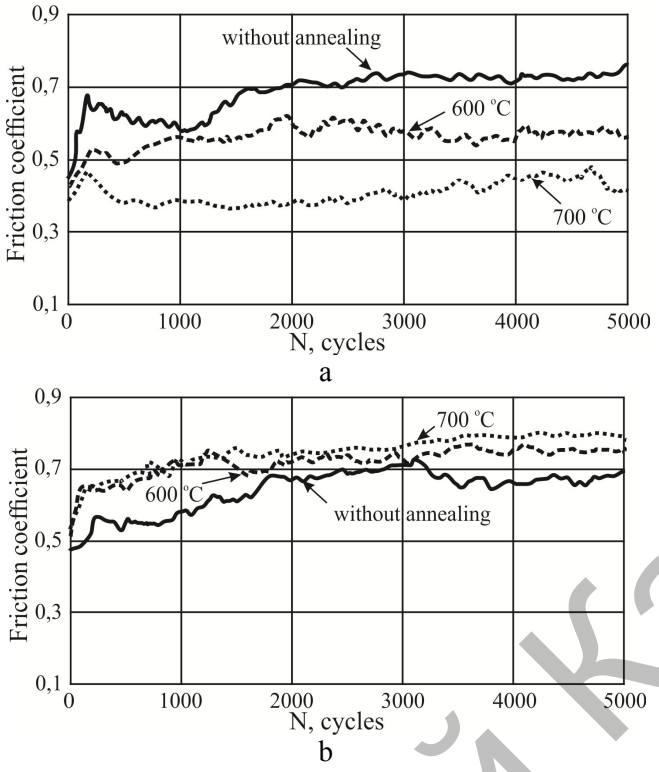

Figure 7. Influence of heat treatment on kinetic dependences of friction coefficient of non-nitrided (a) and nitrided (b) silicon-carbon coatings

In fact, the microhardness, friction, and wear of carbon-based coatings largely depend on the sp^2 / sp^3 ratio of hybridized carbon atoms [23–25]. The surface roughness of carbon coatings can also lead to an increase in the friction and wear coefficients during counterbody motion [23]. In addition to surface roughness, a high degree of chemical and/or adhesive interaction in the slip plane can also adversely affect the coefficient of friction.

On the one hand, the increase in surface energy recorded by us after annealing should contribute to an increase in the adhesive component of the friction force. The main source of adhesive interaction in the case of carbon-based coatings is covalent bonds or free σ-bonds of carbon atoms [2]. This type of bond can cause a very strong adhesive interaction and increase the friction coefficient, especially in the case of non-hydrogenated carbon coatings containing a high number of sp^3-hybridized carbon atoms [26–28].

However, according to the XPS data, the heat treatment of silicon-carbon coatings increases the graphite content, which plays the role of a solid lubricant and helps to reduce the friction coefficient. The high coefficient of friction before heat treatment is explained by the presence of solid phases based on silicon carbide and uneven surface wear during friction [29].

The abrasive action of silicon carbide also explains the higher coefficient of volumetric wear of the counterbody when interacting with the surface of silicon-carbon coatings not subjected to heat treatment.

It was found that silicon-carbon coatings nitriding contributes to the thermal stability of the friction coefficient (Figure 7, b). However, if the friction coefficient of nitrided silicon-carbon coatings does not change significantly, then the coefficient of volume wear of the counterbody when interacting with such coatings raises by increasing annealing temperature. It is explained by the highly dispersed structure of nitrided coatings and the abrasive action of heat-resistant solid interstitial phases based on CN_x and Si_3N_4 compounds present in their composition.

Conclusion

It was shown that bringing nitrogen into the working gas structure ($Ar_{57\,\%}$ + $N_{43\,\%}$) leads to the formation of a highly dispersed structure than using only argon. The influence of annealing in the air on the elemental structure of nitrided and non-nitrided coatings is similar: there is a decrease in carbon concentration and an increase in oxygen concentration. It is due to silicon and carbon oxidation which is followed by carbon and oxygen compounds desorption. It was shown that annealing leads to nitrogen desorption, its content

decreases by 4 times. Apparently, after annealing nitrogen remains only in the bound state in the form of CN_x or Si_3N_4 compounds, which are characterized by high heat resistance.

The analysis of XPS results shows that in addition to the formation of silicon nitride silicon-carbon coatings nitriding contributes to the formation of compounds of the CN_x and $Si_xO_yN_z$ type and increases the content of sp^2-hybridized carbon atoms by 1.25 times, and silicon carbide by almost 2 times. It also prevents from silicon oxidation. High-temperature annealing of both non-nitrided and nitrided silicon-carbon coatings leads to an increase in the content of the graphite phase and silicon oxide. It was shown if the annealing temperature is increased to 700 °C, the proportion of the integral area of N-Si and N-Csp^3 components of the N1s peak of XPS is decreased, and at the same time the proportion of integral area of the component which correlates with N-Csp^2 and Si-O-N simultaneously is increased. This increase is explained primarily by the annealing of the $sp^3 \rightarrow sp^2$ phase transitions, since the increase in the proportion of the integral area of Csp^2 component of the C1s peak is more significant than the change in the proportion of the integral area of Si-O-N component of the Si2p peak.

Silicon-carbon coatings annealing increases the thermal stability of their mechanical properties: the microhardness and friction coefficient during annealing do not change significantly in contrast to non-nitrided coatings. It is due to the presence of heat-resistant compounds CN_x and Si_3N_4 in the coating structure.

Acknowledgments

The research was produced with the financial support of the Belarusian Republican Foundation for Fundamental Research (contract No. T18M-005).

The study was supported by the Ministry of Science and Higher Education of Russia (project/application No. FSFZ-2020–0022).

References

1 Zhumabekov, A.Zh., Ibrayev, N.Kh., Seliverstova, E.V., & Kamalova, G.B. (2019). Preparation and study of electrophysical and optical propertiesof TiO_2-GO nanocomposite material. *Bulletin of the University of Karaganda-Physics, 2 (94),* 54–60, DOI: 10.31489/2019Ph2/54–60

2 Donnet, C. (1998). Recent progress on the tribology of doped diamond-like and carbon alloy coatings: a review. *Surf. Coat. Technol,* 100–101, 180–186, DOI:10.1016/S0257–8972(97)00611–7.

3 Zhumabekov, A.Zh., Ibrayev, N.Kh., Seliverstova, E.V., & Kamalova, G.B. (2019). Preparation and study of electrophysical and optical propertiesof TiO_2-GO nanocomposite material. *Bulletin of the University of Karaganda-Physics, 2 (94),* 54–60, DOI:10.31489/2019Ph2/54–60

4 Chu, P.K. (2006). Characterization of amorphous and nanocrystalline carbon films. *Mater. Chem. Phys, 96,* 253–277, DOI:10.1016/j.matchemphys.2005.07.048.

5 Voevodin, A.A., & Zabinski, J.S. (1998). Superhard, functionally gradient, nanolayered and nanocomposite diamond-like carbon coatings for wear protection. *Diam. Relat. Mater, 7,* 463–467, DOI:10.1016/S0925–9635(97)00214–8.

6 Miao, Yi Ming, Piliptsou, D.G., Rudenkov, A.S., Rogachev, A.V., Xiaohong Jiang, Sun Dongping, Chaus, A.S., & Balmakou, A. (2017). Structure, mechanical and tribological properties of Ti-doped amorphous carbon films simultaneously deposited by magnetron sputtering and pulse cathodic arc. *Diam. Relat. Mater, 77,* 1–9, DOI: 10.1016/j.diamond.2017.05.010

7 Piliptsou, D.G, Rudenkov, A.S., Rogachev, A.V., Xiaohong, Jiang, Lychnikov, P.A., & Emel'yanov, V.A. (2017). XPS study of the structure of nitrogen doped a-C film. *IOP Conf. Ser.: Mater. Sci. Eng,* 168, DOI:10.1088/1757–899X/168/1/012103.

8 Rudenkov, A.S., Rogachev, A.V., Kupo, A.N., Luchnikov, P.A., & Chicherina, N. (2019). The phase composition and structure of silicon-carbon coatings. *Materials Science Forum, 970,* 283–289, DOI: 10.4028/www.scientific.net/MSF.970.283

9 Raveh, A. (2007). Thermal stability of nanostructured superhard coatings: a review. *Surf. Coat. Technol, 201,* 6136–6142, DOI:10.1016/j.surfcoat.2006.08.131.

10 Cloutier, M. (2014). Long-term stability of hydrogenated DLC coatings: Effects of aging on the structural, chemical and mechanical properties. *Diam. Relat. Mater, 48,* 65–72, DOI: 10.1016/j.diamond.2014.07.002.

11 Ferrari, A.C. (2002). Determination of bonding in diamond-like carbon by Raman spectroscopy. *Diam. Relat. Mater, 11,* 1053–1061, DOI:10.1016/S0925–9635(01)00730–0.

12 Shuleiko, D.V., Zabotnov, S.V., Zhigunov, D.M., Zelenina, A.A., Kamenskih, I.A., & Kashkarov, P.K. (2017). Photoluminescence of amorphous and crystalline silicon nanoclusters in silicon nitride and oxide superlattices. *Semiconductors, 51,* 196–202. DOI: 10.1134/S1063782617020208.

13 Li, H. (2004). Zhang The study of bonding composition of CN_x film by thermal degradation method. *Carbon, 42,* 537–545, DOI: 10.1016/j.carbon.2003.12.036.

14 Quirós, C. (2000). Bonding and morphology study of carbon nitride films obtained by dual ion beam sputtering. *Journal of Vacuum Science and Technology A, 18,* 515–523, DOI:10.1116/1.582218.

15 Ronning, C. (1998). Carbon nitride deposited using energetic species: a reviews on XPS studies. *Physical Review B, 58,* 2207–2215, DOI:10.1103/PhysRevB.58.2207.

16 Lubwama, M. (2012). Characteristics and tribological performance of DLC and Si-DLC films deposited on nitrile rubber. *Surf. Coat. Technology, 206,* 4585–4593, DOI: 10.1016/j.surfcoat.2012.05.015.

17 Kusunoki, I., & Igari, Y. (1992). XPS study of a SiC film produced on St(100) by reaction with a C_2H_2 beam, *Applied Surface Science, 59,* 95–104, DOI: 10.1016/0169–4332(92)90293–7.

18 Castanho Mello, S., & Moreno, R. (1998). Characterization of Si_3N_4 powders in aqueous dispersions. *Cerâmica, 44,* 287–288, DOI: 10.1590/S0366–69131998000400006.

19 Nguen, V.L. (2015). N-doped polymer-derived Si(N)OC: The role of the N-containing precursor. *Journal of Materials Research, 30,* 770–781, DOI: 10.1557/jmr.2015.44.

20 Trusso, S., Vasi, C., & Neri, F. (1999). CNx thin films grown by pulsed laser deposition: Raman, infrared and X-ray photoelectron spectroscopy study. *Thin Solid Films, 335–356,* 219–222, DOI: 10.1016/S0040–6090(99)00503–9.

21 Surzhikov, A.P., Peshev, V.V., Pritulov, A.M., & Gyngazov, S.A. (1999). Grain-boundary diffusion of oxygen in polycrystalline ferrites. *Russian Physics Journal, 42,* 490–495, DOI: 10.1007/BF02508222.

22 Chang J.P. (2000). Profiling nitrogen in ultrathin silicon oxynitrides with angle-resolved x-ray photoelectron spectroscopy. *Journal of Applied Physics, 87,* 4449–4455, DOI: 10.1063/1.373090.

23 Donnet, C. (1999). Diamond-like carbon based functionally gradient coatings for space tribology, *Surf. Coat. Technology, 120, 548*–554, DOI:10.1016/S0257–8972(99)00432–6.

24 Evaristo, M., Polcar, T., & Cavaleiro, A (2014). Tribological behavior of W-alloyed carbon based coat-ings in dry and lubricated sliding contact. *Lubrication Science, 26,* 428–439, DOI: 10.1002/ls.1259.

25 Luchnikov, P.A. (2018). Defect formation in fluoropolymer films at their condensation from a gas phase. *IOP Conf. Ser.: Mater. Sci. Eng, 289,* DOI: 10.1088/1757–899X/289/1/012037.

26 Wang, L.L., Wang, R.Y., Yan, S.J., Zhang, R., Yang, B., Zhang, Z.D., Huang, Z.H., & Fu, D.J. (2013). Structure and properties of Mo-containing diamond-like carbon films produced by ion source assisted cathodic arc ion-plating, *Applied Surface Science, 286,* 109–114, DOI: 10.1016/j.apsusc.2013.09.029.

27 Shi, W.L., Wei, X.T., Zhang, W., Wang, Z.G., Dong, C. H., & Li, S. (2017). Developments and applications of diamond-like carbon. *Applied Mechanics and Materials, 864,* 14–24, DOI: 10.4028/www.scientific.net/AMM.864.14.

28 Surzhikov, A.P., Lysenko, E.N., Malyshev, A.V., Vlasov, V.A., Suslyaev, V.I., Zhuravlev, V.A., Korovin, E.Y., & Dotsenko, O.A. (2014). Study of the radio-wave absorbing properties of a lithium-zinc ferrite based composite. *Russian Physics Journal, 57,* 621 — 626.

29 Surzhikov, A., Frangulyan, T., & Ghyngazov, S. (2014). A thermoanalysis of phase transformations and linear shrinkage kinetics of ceramics made from ultrafine plasmochemical $ZrO_2(Y)$-Al_2O_3powders. *Journal of Thermal Analysis and Calorimetry, 115,* 1439–1445 DOI: 10.1007/s10973–013–3455-y

А.С. Руденков, А.В. Рогачев, С.М. Завадский, Д.А. Голосов,
П.А. Лучников, Г.Ю. Дальская, А.Н. Вторушина

Нитридті кремний-көміртек жабындарының құрылымы және қасиеттері

Мақалада азот иондарымен легирлеу кезінде газ тәріздес ортадан алынған кремний-көміртекті жабындардың құрылымдық және физика-механикалық қасиеттері қарастырылған. Рентгендік фотоэлектронды спектроскопия көмегімен жабындарды талдау кремний-көміртекті жабындарды нитриттеу кремний нитридінің және CN_x және $Si_xO_yN_z$ сияқты қосылыстардың түзілуіне ықпал ететіндігін көрсетеді. Sp2-гибридтендірілген көміртек атомдары мен кремний карбиді мөлшерінің 1,5–2 есе артуы кремнийдің тотығуына жол бермейді. Алынған кремний-көміртекті жабындарды термиялық жағу графит фазасы мен кремний оксидінің құрамын арттырады. Азотпен ($Ar_{57\,\%}$ + $N_{43\,\%}$) жұмыс жасайтын газды легирлеу тек аргонды қолданумен салыстырғанда ұсақ дисперсті құрылымның пайда болуына әкелетіні көрсетілген. Ауаны термиялық жағу кезінде кремний мен көміртектің тотығуынан көміртегі мен оттегі қосылыстарының десорбциясының нәтижесінде көміртектің төмен концентрациясы және оттегінің жоғарылауы байқалған. Сонымен қатар, балқыту жабыннан азоттың десорбциясына әкеледі. Кремний-көміртекті жабындарды нитрлеу олардың құрылымының дисперсиясын жоғарылатады, ал CN_X, Si_3N_4 ыстыққа төзімді қосылыстар жабындардың жылуға төзімділігі мен жылуға төзімділігін жақсартады, сонымен қатар үйкеліс бөліктеріндегі микроқаттылық пен үйкеліс коэффициентін арттырады.

Кілт сөздер: көміртекті жабындар, азоттандыру, кремний, фазалық құрам, ион сәулесінің шашырауы, комбинациялық шашырау спектроскопиясы, XPS, микроқаттылық, үйкеліс коэффициенті.

А.С. Руденков, А.В. Рогачев, С.М. Завадский, Д.А. Голосов,
П.А. Лучников, Г.Ю. Дальская, А.Н. Вторушина

Структура и свойства нитридных кремниево-углеродных покрытий

В статье рассмотрены структурные и физико-механические свойства кремний-углеродных покрытий, нанесенных из газовой среды при легировании ионами азота. Анализ покрытий методом рентгеновской фотоэлектронной спектроскопии показывает, что азотирование кремний-углеродных покрытий способствует образованию нитрида кремния и таких соединений, как CN_x и $Si_xO_yN_z$. Установлено, что увеличение содержания sp2-гибридизованных атомов углерода и карбида кремния в 1,5–2 раза предотвращает окисление кремния. Термический отжиг полученных кремний-углеродных покрытий увеличивает содержание графитовой фазы и оксида кремния. Показано, что легирование рабочего газа азотом ($Ar_{57\,\%}$ + $N_{43\,\%}$) приводит к образованию более мелкодисперсной структуры по сравнению с использованием только аргона. Во время термического отжига на воздухе можно наблюдать пониженную концентрацию углерода и повышенную концентрацию кислорода из-за окисления кремния и углерода с последующей десорбцией соединений углерода и кислорода. Кроме того, отжиг приводит к десорбции азота с покрытия. Азотирование кремний-углеродных покрытий увеличивает дисперсию их структуры, а термостойкие соединения CN_x, Si_3N_4 улучшают термостойкость покрытий и повышают микротвердость, а также коэффициент трения в узлах трения.

Ключевые слова: углеродные покрытия, азотирование, кремний, фазовый состав, ионно-лучевое распыление, спектроскопия комбинационного рассеяния, XPS, микротвердость, коэффициент трения.